Technical Report

*Nature Medicine* **14**, 213 - 221 (2008)
Published online: 13 January 2008 | doi:10.1038/nm1684

# Perfusion-decellularized matrix: using nature's platform to engineer a bioartificial heart

Harald C Ott[1], Thomas S Matthiesen[2], Saik-Kia Goh[2], Lauren D Black[3], Stefan M Kren[2], Theoden I Netoff[3] & Doris A Taylor[2,4]

**About 3,000 individuals in the United States are awaiting a donor heart; worldwide, 22 million individuals are living with heart failure. A bioartificial heart is a theoretical alternative to transplantation or mechanical left ventricular support. Generating a bioartificial heart requires engineering of cardiac architecture, appropriate cellular constituents and pump function. We decellularized hearts by coronary perfusion with detergents, preserved the underlying extracellular matrix, and produced an acellular, perfusable vascular architecture, competent acellular valves and intact chamber geometry. To mimic cardiac cell composition, we reseeded these constructs with cardiac or endothelial cells. To establish function, we maintained eight constructs for up to 28 d by coronary perfusion in a bioreactor that simulated cardiac physiology. By day 4, we observed macroscopic contractions. By day 8, under physiological load and electrical stimulation, constructs could generate pump function (equivalent to about 2% of adult or 25% of 16-week fetal heart function) in a modified working heart preparation.**

In the United States alone, nearly 5 million people live with heart failure, and about 550,000 new cases are diagnosed annually. Heart transplantation remains the definitive treatment for end-stage heart failure, but the supply of donor organs is limited. Once a heart is transplanted, individuals face lifelong immunosuppression and often trade heart failure for hypertension, diabetes and renal failure[1]. The creation of a bioartificial heart could theoretically solve these problems. Attempts to engineer heart tissue have involved numerous approaches[2]. Engineered contractile rings and sheets have been transplanted into small animals and have improved ventricular function[3, 4, 5]. The creation of 'thick' (>100–200 μm) cardiac patches has been limited by an inability to create the geometry necessary to support the high oxygen and energy demands of cardiomyocytes at a depth greater than ~100 μm from the surface[2, 6]. The use of channeled cardiac extracellular matrix (ECM) constructs, oxygen carriers and stacked cardiac sheets[4, 7, 8] to improve thickness has reinforced the direct relationship between perfusion and graft size or cell density[6, 9].

To create a whole-heart scaffold with intact three-dimensional geometry and vasculature, we attempted to decellularize cadaveric hearts by coronary perfusion with detergents, which have been shown to generate acellular scaffolds for less complex tissues, by direct immersion[10, 11, 12, 13, 14]. We then repopulated decellularized rat hearts with neonatal cardiac cells or rat aortic endothelial cells and cultured these recellularized constructs under simulated physiological conditions for organ maturation[15]. Ultimately, chronic coronary perfusion, pulsatile left ventricular load and synchronized left ventricular stimulation led to the formation of contractile myocardium that performed stroke work.

## Results

### Perfusion decellularization of cadaveric hearts

To develop a valid perfusion decellularization protocol, we carried out antegrade coronary perfusion of 140 cadaveric rat hearts on a modified Langendorff apparatus and compared the degree of decellularization (that is, removal of DNA and intracellular structural proteins) that resulted from the use of three detergent solutions (**Fig. 1**). The use of SDS (**Fig. 1c,f**) gave better results than did polyethylene glycol (PEG; **Fig. 1a,d**), Triton-X100 (**Fig. 1b,e**) or enzyme-based protocols (data not shown) for full removal of cellular constituents. Antegrade coronary SDS perfusion over 12 h (**Fig. 1c**) yielded a fully decellularized construct. Histological evaluation revealed no remaining nuclei or contractile elements (**Fig. 1g**). DNA content decreased to less than 4% of that in cadaveric heart (**Supplementary Fig. 1** online), whereas the glycosaminoglycan content was unchanged. After perfusion with Triton-X100 (ref. **16**) and washing, SDS levels in the decellularized myocardium could not be differentiated from zero in a quantitative assay (**Supplementary Fig. 1**).

**Figure 1: Perfusion decellularization of whole rat hearts.**

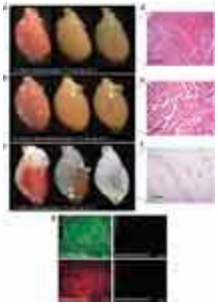

(**a**–**c**) Photographs of cadaveric rat hearts mounted on a Langendorff apparatus. Ao, aorta; LA, left atrium; LV, left ventricle; RA, right atrium; RV, right ventricle. Retrograde perfusion of cadaveric rat heart using PEG (**a**), Triton-X-100 (**b**) or SDS (**c**) over 12 h. The heart becomes more translucent as cellular material is washed out from the right ventricle, then the atria and finally the left ventricle. (**d**,**e**) Corresponding H&E staining of thin sections from LV of rat hearts perfused with PEG (**d**) or Triton-X-100 (**e**), showing incomplete decellularization. Hearts treated with PEG or Triton-X-100 retained nuclei and myofibers. Scale bars, 200 μm. (**f**) H&E staining of thin section of SDS-treated heart showing no intact cells or nuclei. Scale bar, 200 μm. All three protocols maintain large vasculature conduits (black asterisks). (**g**) Immunofluorescent staining of cadaveric and SDS-decellularized rat heart thin sections showing the presence or absence of DAPI-positive nuclei (purple), cardiac α-myosin heavy chain (green) or sarcomeric α-actin (red). Nuclei and contractile proteins were not detected in decellularized constructs. Scale bars, 50 μm.

**Full size image (97 KB)**

### Properties of the decellularized construct

Collagens I and III, laminin and fibronectin (**Fig. 2a**) remained within the thinned, decellularized heart matrix. The fiber composition (weaves, struts and coils) and orientation of the myocardial ECM were preserved, whereas cardiac cells were removed (**Fig. 2b**), resulting in compressed constructs. Within the retained ventricular ECM, we saw intact vascular basal membranes without endothelial or smooth muscle cells. A thin layer of dense epicardial fibers beneath an intact epicardial basal lamina was retained. Fiber orientation and composition was also preserved in the decellularized aortic wall and aortic valve leaflet (**Fig. 2c**). The aortic valve remained competent (at a constant coronary perfusion pressure of 77.4 mm Hg; see **Supplementary Fig. 2a** online) as confirmed by Evans blue perfusion. A competent tricuspid valve was observed after heterotopic transplantation (**Supplementary Fig. 2b**).

**Figure 2: Composition and characteristics of decellularized rat heart tissue.**

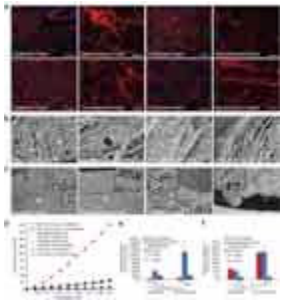

(**a**) Immunofluorescence micrographs of control cadaveric and decellularized rat heart thin sections. No (purple) DAPI staining of intact nuclei was detected in decellularized heart; the ECM components collagen I and III, laminin and fibronectin were preserved. Fluorescence intensity appears to increase in decellularized heart images, presumably owing to the compression of matrix that follows the removal of cells. Scale bars, 50 μm. (**b**) Scanning electron micrographs (SEM) of cadaveric and decellularized left ventricular (LV) and right ventricular (RV) myocardium shows the presence of myofibers (mf) in the cadaveric heart that are missing in the decellularized matrix. Characteristic weaves (w), coils (c), struts (s) and dense epicardial fibers (epi) are retained. Scale bars, 50 μm. (**c**) SEM of cadaveric and decellularized aortic wall and aortic valve leaflet. The collagen and elastin fibers in the aortic wall are maintained and the aortic valve leaflets are preserved, but cells throughout all tissue layers were removed. a, aortic side; c, circumferential fibers; ec, endothelial cells; I, intima; M, media; v, ventricular side. Scale bars for main images 50 μm; for inserts, 10 μm. (**d**) Engineering stress-strain curves in the longitudinal and circumferential directions from a representative sample of normal rat LV, decellularized rat LV and fibrin gel. (**e,f**) Tangential modulus (**e**) in kPa and membrane stiffness (**f**) in kN/m of cadaveric rat LV, decellularized rat LV and fibrin gel at 40% strain.

**Full size image (95 KB)**

In equibiaxial mechanical testing, cadaveric and decellularized rat heart samples were highly anisotropic with respect to their stress-strain behavior (**Fig. 2d**) compared to fibrin gel controls. For cadaveric left ventricles, the stress at 40% strain varied between 5 and 14 kPa longitudinally and 15 and 24 kPa circumferentially. In both cadaveric and decellularized left ventricles, the circumferential direction was stiffer than the longitudinal direction. To compare the stress-strain properties, we calculated a tangential modulus at 40% strain in both the circumferential and longitudinal directions (**Fig. 2e**). Decellularized samples had a significantly higher modulus than cadaveric rat ventricles or fibrin gel (**Fig. 2e**). Tangential moduli in the two directions for cadaveric and decellularized left ventricles also differed. The values of the tangential modulus of the decellularized tissues are only slightly greater than the values of Young's modulus for purified elastin (~600 kPa) and less than that of Young's modulus for a single collagen fiber (5 MPa), placing the values in an expected range. When adjusted for thickness, membrane stiffness at 40% strain did not differ between the decellularized and cadaveric tissues (**Fig. 2f**). However, both decellularized and cadaveric tissue were stiffer than fibrin gels[17].

Direct perfusion of the coronary vasculature of both cadaveric and decellularized hearts (**Fig. 3a**) with red Mercox resin showed that both the larger cardiac vessels and the smaller third- and fourth-level branches were patent.

Functional perfusion was confirmed by heterotopic transplantation of a decellularized rat cardiac construct (**Fig. 3b**) with reperfusion of the construct upon release of the clamped aorta of the host (**Fig. 3b** and **Supplementary Movie 1** online). The arterial and venous basement membranes remained intact (**Fig. 3c**), coronary ostia retained their luminal diameter and shape (**Fig. 3d**) and endothelial cells or nuclei were absent (**Fig. 3d**).

**Figure 3: Vascular architecture of decellularized rat heart tissue.**

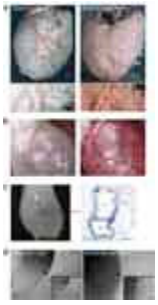

(**a**) Macroscopic (upper row; scale bar, 1,000 μm) and microscopic views (lower row; scale bar, 250 μm) of coronary corrosion casts of cadaveric and decellularized whole adult rat hearts. (**b**) Heterotopically transplanted decellularized whole rat heart before (left) and shortly after (right) unclamping of the host aorta (see **Supplementary Movie 1**). (**c**) SDS-decellularized heart and corresponding Masson's trichrome–stained microscopic section of left ventricular myocardium showing a large artery (A) and vein (V). Scale bar, 250 μm. (**d**) SEM of freshly isolated and decellularized aortic root and left main coronary artery ostium. The left main coronary artery and the aortic root architecture were preserved in decellularized hearts, but the endothelial cell cobblestone pattern (black arrows) seen in the cadaveric sample (insert, left panel) was absent after decellularization (insert, right panel) despite the preservation of a smooth basal lamina (black arrowheads). Main panels: scale bars, 200 μm; inserts: scale bars, 100 μm.

**Full size image (98 KB)**

### Recellularization of decellularized cadaveric hearts

To test whether perfusion culture and physiological stimulation would support tissue formation and maturation to a greater degree than nonperfused two-dimensional culture, we mounted recellularized whole rat hearts into a bioreactor that provided coronary perfusion with oxygenated culture medium (**Fig. 4a,b**), and we compared developed tissue contractility after 8–10 d with that of recellularized cardiac ECM sections that had been maintained in standard two-dimensional nonperfused tissue-culture dishes (**Fig. 4c**). Immediately before mechanical testing, we sectioned recellularized whole hearts to obtain comparable tissue samples.

**Figure 4: Formation of a working perfused bioartificial heart-like construct by recellularization of decellularized cardiac ECM.**

(**a**) Schematic of working heart bioreactor showing cannulation of left atrium and ascending (asc.) aorta. The heart is exposed to physiological preload, afterload and intraventricular pressure and is electrically stimulated at 5–20 V. Oxygenated medium containing serum and antibiotics enters through the left atrium and exits through the aortic valve. Pulsatile distention of the LV and a compliance loop attached to the ascending aorta provide physiological coronary perfusion and afterload. Coronary perfusate (effluent) exits through the right atrium. (**b**) Top, recellularized whole rat heart at day 4 of perfusion culture in a working heart bioreactor. Upper insert, cross-sectional ring harvested for functional analysis (day 8); lower insert, Masson's trichrome staining of a ring thin section showing cells throughout the thickness of the wall. Scale bar, 100 μm. Bottom, force generation in left ventricular rings after 1-Hz (left) and 2-Hz (right) electrical stimulation. (**c**) Top, recellularized rat heart rings cultured for up to 10 d without perfusion. Scale bar, 250 μm. Upper insert: microscopic view of cross-sectional ring showing rhythmic contractions at day 9 (**Supplementary Movie 2**); lower insert: Masson's trichrome staining of ring thin section harvested for force generation studies after 10 d *in vitro* (scale bar, 50 μm). Bottom, force generation in non-perfused rings at day 10, after 1-Hz (left) or 2-Hz (right) electrical stimulation. (**d**) Left, representative functional assessment tracing of decellularized whole heart construct paced in a working heart bioreactor preparation at day 0. Real-time tracings of ECG, aortic pressure (afterload) and left ventricular pressure (LVP) are shown. Center, paced recellularized heart construct on culture day 4 with pump turned off (**Supplementary Movies 3** and **4**). Right lateral view (top) and anterior view (bottom) show physiological landmarks, including RV and LV. Tracing shows quantification of a region of movement in the beating preparation (**Supplementary Movies 3** and **4**). Right, tracings of ECG (red), aortic pressure (afterload) and LVP of the paced construct on day 8 after recellularization and on day 8 after stimulation with physiological (~50–100 μM) doses of phenylephrine. (**e**) Summary of day 8 function in recellularized working heart preparation. Maximal developed LVP and d*P*/d*t* max obtained by day 8 in working heart bioreactor preparations.

**Full size image (94 KB)**

After 4 d in two-dimensional culture, we saw contracting cell patches that progressed to synchronously contracting tissue rings by day 9 (**Supplementary Movie 2** online). Both sets of rings could be electrically paced at 1 Hz or 2 Hz (**Fig. 4b,c**) up to a frequency of 4 Hz. Both reseeded constructs could generate force comparable to the maximal force for rings created using artificial ECM[2]. In both constructs, increases in stimulation frequency decreased contraction twitch force; at both 1 and 2 Hz, the contraction twitch force for the perfusion-maintained ring was ~300 and 800% of that of the cell-seeded decellularized ring. As in artificial ECM constructs lacking perfusion[2, 6], we could not generate viable cardiac muscle with a diameter greater than ~50 μm unless the construct was perfused, in

which case we obtained myofibers of ~250-μm (**Fig. 4b**) to 1.1-mm thickness.

### Whole-heart experiments

We mounted decellularized rat hearts ($n$ = 8) in a bioreactor and seeded them with freshly isolated neonatal cardiac cells through intramural injection. We adjusted sterile organ-culture conditions (**Fig. 4a**) to provide simulated systolic and diastolic medium flow through pulsatile antegrade left heart perfusion and a circuit of coronary flow through a left atrial cannula. Perfusate was ejected passively through the aortic valve into a compliance loop that allowed afterload adjustment. Pressures were adjusted to allow closure of the aortic valve between each pulse in order to provide pulsatile coronary perfusion (day 1, 7 ml/min) during simulated diastole and ventricular relaxation. Over the course of culture, pulsatile left ventricular distension (simulated end-diastole) was gradually increased by adjusting the preload (1–12 mm Hg) and afterload (1–60 mm Hg). Electrical stimulation (pacing) was provided through epicardial leads (1 Hz, 5–20 V, 2 ms). Perfused organ culture was maintained for 8–28 d. By day 8 after cell seeding, heart constructs showed electric and contractile responses to single paces (**Supplementary Movies 3** and **4** online). At day 8, we performed in-depth analysis of left ventricular pressure (LVP) and contractile function as we gradually increased stimulation frequency from 0.1 Hz to 10 Hz or administered phenylephrine (**Fig. 4d**). Stimulated contractions at day 8 (**Fig. 4d**) caused a corresponding increase in LVP and a recordable repolarization. When repeated pacing was less than 4 Hz, contractile force remained constant at ~2.4 mm Hg (~2% of adult rat heart function and 25% of 16-week fetal human heart function[18]). When stimulation frequency was increased beyond 4 Hz, contractile force decreased (**Fig. 4d**), as found in the ring experiments. We observed spontaneous rhythmic depolarizations and contractions for up to 340 s after single external electrical pulses (data not shown). These could be suppressed by increasing pacing frequency beyond 1 Hz. Maximum capture rate was approximately 5 Hz, consistent with the refractory period of mature rat myocardium (250 ms). We obtained functional measurements (maximal LVP and maximal change in pressure over change in time ($dP/dt$ max)) in 5 of 8 constructs (**Fig. 4e**). Three preparations were stopped early because of infection.

On histological analysis, the average recellularization per cross-section of scaffold (at day 8) in the final two preparations was 33.8 ± 3.4% proximally (1–2 mm) to injection sites, and it decreased distally. Recellularization (**Fig. 5**) of previously decellularized constructs was greatest in the area of injection (left ventricular mid-wall) when compared to the remote areas (left ventricular base and apex and right ventricle). By day 8, there were areas of confluent cellularity approximately 1 mm thick (**Fig. 5a**). Viability was >95% throughout the entire thickness (0.5–1.1 mm). Sarcomeric α-actin and cardiac myosin heavy chain (**Fig. 5a,b**) were expressed throughout the left ventricle, in some areas accompanied by cells that were positive for von Willebrand factor (vWF; **Fig. 5b**). The small number of vWF-positive cells was seen in the absence of reperfusion of endothelial cells and presumably arose from endothelial components derived from the injected neonatal cells. Immature cross-striated contractile fibers began to organize by days 8–10, as did expression of connexin-43 (**Fig. 5c**). Synchronous paced contraction of the construct as early as day 4 (**Supplementary Movies 3** and **4**) indicates that these connections were functional.

**Figure 5: Histological analysis of recellularized rat heart constructs.**

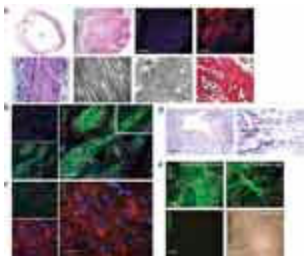

(**a**) Recellularized whole heart. Top left, recellularized heart at day 8 in cross-section. Top, second panel, H&E staining of ventricular wall (scale bar, 1,000 μm) to show graft thickness; third panel, corresponding immunofluorescent staining for TUNEL (scale bar, 250 μm); top right, immunofluorescent staining for sarcomeric α-actin (scale bar, 250 μm). Bottom left, Z-bands within recellularized tissue (H&E, scale bar, 20 μm); bottom, second panel, TEM (scale bar, 200 nm). Bottom, third panel, sarcomeres observed longitudinally (black arrowheads) and in cross section (red arrowheads) within recellularized LV by TEM (scale bar, 500 nm). Bottom right,

relatively mature regions of cardiocytes at day 10 (Masson's trichrome; scale bar, 20 μm). (**b**) Co-staining for MHC and vWF (red). White arrows, vWF-positive regions; asterisks, small channels in recellularized construct. Scale bar, 100 μm. Inset, striated MHC-positive cell. Scale bar, 10 μm. (**c**) Co-staining for MHC and connexin-43, showing expression of gap-junction associated protein in recellularized heart. Scale bar, 20 μm. (**d**) H&E staining of re-endothelialized decellularized rat heart matrix after 7 d in perfused organ culture. Endothelial cells are evident throughout what appear to be small and large vessels (left, scale bar 250 μm; right, scale bar 50 μm). (**e**) Re-endothelialized rat heart matrix perfused with CMFDA. Vessels in LV anterior wall surface (upper right), and cobblestone appearance of confluent endothelial cells observed in *en face* view of LV endocardial surface (upper left). Control construct without CMFDA uptake (lower left). Phase-contrast image of control construct (lower right). Scale bars, 100 μm.

**Full size image (75 KB)**

**Re-endothelialization of decellularized construct**

Rat aortic endothelial cells were seeded onto decellularized cardiac ECM by media perfusion. After 7 d, endothelial cells formed single layers in both larger and smaller coronary vessels throughout the wall (**Fig. 5d**), which could metabolize 5-chloromethylfluorescein diacetate (CMFDA) dye (**Fig. 5e**); simultaneously, the ventricular cavities were re-endothelialized (**Fig. 5e**). Decellularized tissue before reseeding (control) showed no $CMFDA^+$ cells (**Fig. 5e**). At day 7, the average cellularity was 550.7 ± 99.0 endothelial cells per $mm^2$ on the endocardial surface and 264.8 ± 49.2 endothelial cells per $mm^2$ within the vascular tree.

## Discussion

We have met three important milestones that are required to engineer a bioartificial heart: engineering of a construct to provide architecture, population of such a construct with an appropriate cell composition, and maturation of this construct to develop nascent pump function. Immersion decellularization has been used previously to create scaffolds in various thin (nonperfused) cardiovascular tissues including vessel wall[19], pericardium[20, 21] and valve leaflets[22, 23]. Decellularization of whole heart, however, has not been reported until now. Using perfusion decellularization, we produced a complex, biocompatible cardiac ECM scaffold with a perfusable vascular tree, patent valves and a four-chamber-geometry template for biomimetic tissue engineering. Reseeding of decellularized heart was possible both by intramural injection of cardiac-derived cells and by perfusion of endothelial cells into the vascular conduits. The recellularized construct was contracting and drug responsive after 8 d of culture. With sufficient maturation, and given the further ability to reseed its inherent vascular architecture and interior with endothelial cells, this organ could become transplantable either in part (for example, as a ventricle for congenital heart disease such as hypoplastic left heart syndrome) or as an entire donor heart in end-stage heart failure. Though the current study is limited to rat hearts, this approach holds promise for virtually any solid organ. Although it is beyond the scope of the current study, we successfully applied perfusion decellularization to porcine heart (**Supplementary Fig. 3** online), showing that this technology can be scaled to hearts of human size and complexity. We have also applied this technique to a variety of mammalian organs including lung, liver, kidney and muscle. Ongoing studies are directed toward optimizing reseeding strategies to promote the dispersion of cells throughout the construct, *in vitro* conditions required for organ maturation, and the choice of stem or progenitor cells necessary to generate either autologous or off-the-shelf bioartificial solid organs for transplantation.

# Methods

**Perfusion decellularization of rat hearts.**

All rat experiments were performed in accordance with US Animal Welfare Act and institutional guidelines and were approved by the Institutional Animal Care and Use Committee at the University of Minnesota. We killed male 12-week-old F344 Fischer rats (Harlan Labs) with 100 mg/kg ketamine (Phoenix Pharmaceutical) and 10 mg/kg xylazine (Phoenix Pharmaceutical) injected intraperitoneally. After systemic heparinization (American Pharmaceutical Partners) through the left femoral vein, a median sternotomy allowed us to open the pericardium. We then removed the retrosternal fat body, dissected the ascending thoracic aorta and ligated its branches. After transecting the caval and pulmonary veins, the pulmonary artery and the thoracic aorta, we removed the heart from the chest. A prefilled 1.8-mm aortic cannula (Radnoti Glass) inserted into the ascending aorta allowed retrograde coronary perfusion (Langendorff). Heparinized PBS (HyClone) containing 10 μM adenosine at a coronary perfusion pressure of 77.4 mm Hg for 15 min followed by 1% SDS (Invitrogen) in deionized water for 12 h served as the perfusate. This was followed by 15 min of deionized water perfusion and 30 min of perfusion with 1% Triton-X100 (Sigma) in deionized water. We used antibiotic-containing PBS (100 U/ml penicillin-G; Gibco), 100 U/ml streptomycin (Gibco) and amphotericin B (Sigma) to perfuse the heart for 124 h.

**Isolation and preparation of rat neonatal cardiocytes.**

We sedated specific pathogen–free Fischer-344 neonatal (1–3-d-old) pups (Harlan Labs) with 5% inhaled isoflurane (Abbott Laboratories), sprayed them with 70% ethanol (Aaron Industries) and performed a rapid sternotomy in a sterile fashion. We excised the hearts and placed them immediately into 50-ml conical tubes (on ice) containing 30 ml HBSS (Reagent 1, Worthington Biochemical), removed the supernatant and washed whole hearts once with cold HBSS by vigorous swirling. We transferred the hearts to a 100-mm culture dish containing 5 ml cold HBSS, removed the connective tissue and minced the remaining tissue into pieces of smaller than 1 $mm^3$. We added HBSS to bring the total plate volume to 9 ml, and added an additional 1 ml trypsin (Reagent 2, Worthington kit) to a final concentration of 50 μg/ml. We incubated plates overnight at 5 °C. Next, we added trypsin inhibitor (Reagent 3, Worthington kit) reconstituted with 1 ml HBSS to each 50-ml conical tube and gently mixed. We oxygenated the tissue for 60–90 s by passing air over the liquid surface and then warmed it to 37 °C, after which we added collagenase (300 U/ml, Reagent 4, Worthington kit) reconstituted with 5 ml Leibovitz L-15 (Worthington Biochemical). We placed the tissue in a 37 °C shaker bath for up to 45 min. Next, we triturated the tissue to release cells and strained it through a 0.22-μm filter (Corning). We washed the tissue in 5 ml L-15 medium, triturated it a second time and collected it in the same 50-ml conical tube. We incubated the resulting cell solution at 20–25 °C for 20 min and centrifuged it at 50*g* for 5 min at 20–25 °C to pellet cells. We removed the supernatant and gently resuspended cells in the desired volumes of neonatal-cardiomyocyte medium (see below).

**Media and solutions.**

We sterile-filtered (0.22-μm filter) all media and kept them in the dark at 5 °C before use. We used Leibovitz L-15 (Worthington Biochemical) medium for tissue processing only. To make Worthington Leibovitz L-15 medium, we reconstituted Leibovitz medium powder in 1 liter of cell culture–grade water according to the manufacturer's recommendations. To make neonatal-cardiomyocyte medium, we supplemented Iscove's Modified Dulbecco's Medium (Gibco) with 10% FBS (HyClone), 2% horse serum (Gibco), 100 U/ml penicillin-G (Gibco), 100 U/ml streptomycin (Gibco), 2 mmol/l L-glutamine (Invitrogen), 0.1 mmol/l 2-mercaptoethanol (Gibco), 1.2 mM CaCl (Fisher Scientific) and 0.8 mM MgCl (Sigma). We used neonatal-cardiomyocyte medium in all ECM recellularization experiments that involved neonatal cardiomyocytes.

**Biaxial passive mechanical properties.**

We cut cross-shaped pieces of myocardial tissue from the left ventricles of rats so that the center area was approximately 5 mm × 5 mm and the axes of the cross were aligned with the circumferential and longitudinal directions of the heart. We measured the initial thicknesses of the cadaveric tissue crosses with a micrometer and found them to be 3.59 ± 0.14 mm in the center of the tissue cross. We also cut crosses from decellularized rat left ventricular tissue in the same orientation and with the same center area size. The initial thickness of the decellularized samples was 238.5 ± 38.9 μm. In addition, we tested the mechanical properties of fibrin gels, another tissue engineering scaffold used in engineering vascular and cardiac tissue. We cast fibrin gels into cross-shaped molds with a final concentration of 6.6 mg of fibrin per ml. The average thickness of the fibrin gels was 165.2 ± 67.3 μm. We attached all samples to a biaxial mechanical testing machine (Instron) with clamps, submerged them in PBS and stretched them equibiaxially to 40% strain. To probe the static passive mechanical properties accurately, we stretched the samples in increments of 4% strain and allowed them to relax at each strain value for at least 60 s. We converted forces to engineering stress by normalizing the force values with the cross-sectional area in the specific axis direction (5 mm × initial thickness). We calculated engineering strain as the displacement normalized by the initial length. To compare the data between the two axes as well as between sample groups, we calculated a tangential modulus as follows:

$$\text{tangential modulus} = (T(\varepsilon = 40\%\ \text{strain}) - T(\varepsilon = 36\%\ \text{strain}))/4\%\ \text{strain}$$

where $T$ is engineering stress and $\varepsilon$ is engineering strain. We averaged the values for the tangential modulus and compared them between the two axes (circumferential and longitudinal) as well as between groups.

**Recellularization of decellularized rat hearts.**

After 124 h of PBS perfusion, we cannulated the atrium and ascending aorta with sterile 16- or 18-gauge cannulae (Radnoti Glass) and sutured sterile stimulation electrodes to the aortic and atrial cannulae and to the apex of the heart. We then mounted the heart in the working-heart bioreactor and perfused it with 37 °C oxygenated cell medium for 24 h at an atrial flow rate of 20 ml/min and a coronary flow rate of 6 ml/min to establish the presence of nutrients and a physiological pH in the ECM seeding bed and to confirm vascular and ventricular integrity and valve function before cell injection. The working-heart bioreactor was based on a water-jacketed working-heart system (Radnoti). We measured preload and afterload with two SP844 Pressure Transducers (Memscap) and measured inflow and outflow with two M-1500 Ultrasonic Flowmeters (Malema Sensors). We recorded all measurements through a Powerlab 16-channel data acquisition system (AD Instruments) connected to a desktop computer using Chart 5.3 (AD Instruments), and we recorded 30-s datasets every 15 min throughout the culture period. For cell seeding, we delivered 50–75 × $10^6$ cells (neonatal cardiomyocytes, fibrocytes, endothelial cells and smooth muscle cells) suspended in PBS through five injections of 200 μl each in the anterior left ventricle with a 27-G needle and a 1-cc tuberculin syringe. Quantification of cell number in the effluent from the myocardium immediately after injection showed a loss of approximately 46% of the cells within 20 min. For nonperfused ring culture, we then sectioned the heart into four ventricular cross sections. We placed the resulting rings into 22-mm cell culture plates in neonatal-cardiomyocyte medium and maintained them under regular cell-culture conditions (37 °C, 60% $H_2O$ and 5% $CO_2$). In the initial studies, we dismounted the heart for 15 min to inject cells. In the more recent whole-heart studies, we performed injections during retrograde perfusion. The heart remained in the sealed bioreactor for whole-heart organ culture, and we initiated automated recording of flow and pressure monitoring (30 s every 15 min). We administered no electrical stimulation in the first 24 h; starting on day 1, we applied 10-ms pulses of 5 V with a Grass SD-9 stimulator (Grass Medical Instruments) through epicardial leads. We continuously oxygenated the perfusate in a bubble oxygenator (Radnoti Glass) and changed this medium every 24 h.

**Re-endothelialization of decellularized rat heart.**

We prepared decellularized heart matrix as described above. After placing the matrix in a bioreactor vessel, thus

allowing closed-circuit retrograde perfusion through the aorta, we introduced approximately $2.0 \times 10^7$ rat aortic endothelial cells (VEC Technologies) into the heart matrix by direct infusion into the patent aorta. After a 45-min static period to allow for attachment, we restarted perfusion and continued it for the 1-week duration of the culture. We maintained culture conditions by placing the entire system in a tissue-culture incubator. In addition to the 5% $CO_2$ atmosphere in the incubator, we injected humidified carbogen (5% $CO_2$, 95% $O_2$) into the medium reservoir. At the end of the culture period, we treated hearts with CellTracker Green (CMFDA, Molecular Probes) according to the manufacturer's instructions. Briefly, we prepared a 10-mM stock solution by dissolving the product in DMSO (Sigma Chemical), and then diluted it in serum-free medium to a 10 μM working concentration. We perfused the culture with this mixture for 45 min at which time we restored growth medium (MCDB-131 Complete, VEC Technologies) for a further 45 min. At the end of the staining protocol, we fixed the culture by perfusion with 10% formalin. As a negative control, we treated heart matrix identically, with the exception of the addition of cells. We dissected the left ventricular wall, placed it on a glass slide and photographed it with an inverted fluorescence microscope. We then embedded the heart in paraffin for thin sectioning. We assessed the density of cells after 1 week of culture by evaluating 5-μm sections with DAPI-containing mounting medium (Vector Laboratories). We quantified nuclei in approximately 25 random fields from 4–6 random, short-axis sections throughout the heart. The number of visible nuclei was factored for the square area of tissue visible in each field with US National Institutes of Health ImageJ software.

**Functional assessment of contractile force of cross-sections.**

To evaluate the force of contraction of the recellularized myocardial tissue, we looped one ring of the recellularized heart around a post attached to a force transducer (60-2994 Research Isometric Transducer, Harvard Apparatus) on one end and looped the other end around a post fixed in a custom-made bath. We connected the force transducer to a data acquisition card (DAQCard AI-16XE-50, National Instruments) and recorded all data using a custom-made LabVIEW program (National Instruments). We next mounted the bath onto a translating rack-and-pinion stage (NT56-337, Edmund Optics), which we used to change the amount of preload on the ring by adjusting the distance between the force transducer post and the post in the bath. Once the ring was set around the two posts, we filled the bath with neonatal cardiomyocyte medium and placed the test stand containing the force transducer and the bath inside a 37 °C tissue-culture incubator on a shock-absorbent material to reduce the amount of vibration affecting the measurement. To ensure contraction, we paced the ring with a custom-built stimulator comprising an amplifier (Model 603, Trek) and a custom LabVIEW program designed to generate the stimulating signal (National Instruments). The leads from the stimulator ended in tungsten stimulating microelectrodes (563420, A-M Systems). We positioned one electrode in direct contact with the ring and the other in the bath ~1 cm away. We paced the ring with a 100-ms-long square wave pulse of amplitude 100 V and at frequencies of 1 and 2 Hz.

**Whole working-heart measurements on recellularized heart.**

We obtained video images of the recellularized heart on day 4, 6 or 8 after injection of cells. We performed functional assessment on day 8 *in vitro*. We inserted a microtip pressure catheter (Millar Instruments) into the left ventricle through the left atrial cannula and electrically stimulated the heart with a Grass SD9 stimulator (Grass Medical Instruments), through one silver electrode sutured to the apex and one electrode connected to the left atrial cannula (ADInstruments), with frequencies of 0.1–10 Hz. We monitored LVP and recorded live video with a PixeLink-A472 video camera. We estimated heart movement from video with 0.25-pixel resolution by using cross-correlation between frames. We calculated cross-correlation between subsequent frames for a small section of the region (colored squares). For each frame, we converted the region of interest to grayscale and leveled and then calculated a two-dimensional Fourier transform[24]. Using the correlation theorem from Fourier theory to calculate the cross correlation, we multiplied the Fourier transform of each frame by the complex conjugate of the Fourier transform from the subsequent frame[25]. The resulting matrix was padded to make an array 4 times larger and then

inverse transformed to make cross-correlation with sub-pixel resolution. We measured movement between frames as the Cartesian distance between the peak in the cross-correlation and the origin. We integrated movement between frames to obtain absolute movement, and then low-pass filtered at 1.25 Hz, using an eight-pole Butterworth filter, to remove drift. To preserve the sign of the movement, we multiplied the absolute movement by the sign of the movement in the *y* direction. This method could measure only movement in the plane of focus and therefore provides only a lower bound estimate. We used MATLAB (MathWorks) to perform all calculations.

**Heterotopic heart transplantation.**

We decellularized donor hearts as described. We anesthetized recipient rats (RNU Nude) with sodium pentobarbital (60 mg/kg intraperitoneally). A midline incision in the abdominal wall exposed the descending aorta and inferior vena cava. We performed an end-to-side anastomosis of the donor heart's ascending aorta and left pulmonary artery to the recipient rat's abdominal aorta and vena cava, respectively, using 9-0 suture as described[26]. We heparinized the recipient rat before transplant with continued anticoagulative therapy (sodium heparin at 100 international units (IU)/kg twice on the day of transplant and 200 IU subcutaneously for the next 2 d) and Coumadin (0.25 mg/kg/d) in drinking water for the following 4–7 d.

**Histology and immunofluorescence.**

We fixed, paraffin-embedded and sectioned recellularized hearts and cell-seeded rings following standard protocols. We cut hearts into 5-μm sections, stained them with Masson's trichrome stain following the manufacturer's instructions (Gomori, procedure HT10, Sigma-Aldrich) and photographed the sections on a Nikon Eclipse TE200 microscope (Fryer). We performed antigen retrieval on paraffin-embedded tissue (recellularized tissue), but not on frozen sections, (decellularized tissue) as follows: we de-waxed paraffin sections and rehydrated them by two changes of xylene for 5 min each, followed by a sequential alcohol gradient and rinsing in cold running tap water. We then placed slides into antigen retrieval solution (10 mM sodium citrate, 0.05% Tween-20, pH 6.0) and heated them until the temperature reached 95–100 °C for 30 min. We allowed the slides to cool for 20 min at room temperature and rinsed them twice in 1 × PBS. We fixed frozen sections with 4% paraformaldehyde (Electron Microscopy Sciences) in 1 × PBS (Mediatech) for 15 min at room temperature before staining. We blocked slides with 4% normal goat serum (goat serum G 9023, Sigma-Aldrich) in 1 × PBS for 30 min at room temperature. We sequentially incubated slides for 1 h at room temperature with diluted primary and secondary antibodies. Between each step, we washed slides three times (5–10 min each) with 1 × PBS. We used primary antibody to cardiac myosin heavy chain (rabbit polyclonal IgG, sc-20641, Santa Cruz Biotechnology; and mouse monoclonal IgG1, NB300-284, Novus Biologicals) at 1:40 and 1:100 dilutions, respectively, in blocking buffer; antibody to vWF (rabbit polyclonal IgG, F3520, Sigma-Aldrich) at a 1:100 dilution in blocking buffer; and antibody to connexin-43 (mouse monoclonal IgM, C8093, Sigma-Aldrich) and antibody to α-sarcomeric actin (mouse monoclonal IgM, A2172, Sigma-Aldrich) at a 1:500 dilution in blocking buffer. For secondary antibodies, we used Alexa Fluor 488–conjugated goat antibodies to mouse IgM (A-21042, Molecular Probes) and to mouse IgG (A-11001, Molecular Probes) and Alexa Fluor 568–conjugated goat antibody to rabbit IgG (A-11011, Molecular Probes) at 1:200 dilutions in blocking buffer. We covered slides with cover glass (Fisherbrand 22 mm × 60 mm) in hardening mounting medium containing DAPI (Vectashield, Vector Laboratories). We recorded images with ImagePro Plus 4.5.1 (Mediacybernetics) on a Nikon Eclipse TE200 inverted microscope (Fryer). For apoptotic cell detection, we used a deoxynucleotidyl TUNEL assay (APO-BrdU TUNEL Assay Kit, Molecular Probes), following the manufacturer's instructions. Briefly, after washing with 1 × PBS for 15 min at room temperature, we treated sections with diluted proteinase K diluted 1:100 in 10 mM Tris, pH 8 (Invitrogen) at room temperature for 10 min. We then dipped the slides 2–3 times into a beaker of 1 × PBS. Between each step, we carefully dried the glass slide around the specimen. We blocked endogenous peroxidase with 3% $H_2O_2$ (Aaron Industries) for 10 min at room temperature. We rinsed the slide with 1 × PBS and incubated it with 0.2% cacodylic acid (Molecular Probes) for 20 min at room temperature. We then incubated the specimens at

room temperature with DNA Labeling Solution (Molecular Probes) for 90 min in a humid chamber. BrdU was added to the terminal deoxynucleotidyl transferase reaction to label the break sites. After rinsing with PBS at room temperature, we incubated the slide with 3% BSA (Sigma-Aldrich) in 1 × PBS (as blocking buffer) for 10 min at room temperature. The DNA fragments labeled with the BrdU were then allowed to bind an antibody to BrdU conjugated to Alexa Fluor 488 fluorescent dye for 90 min at room temperature. We counterstained the specimen with DAPI (Vectashield, Vector Laboratories). Apoptotic nuclei were defined as positive when showing a green color; cells without DNA fragmentation show only blue nuclear staining.

**Scanning electron microscopy and transmission electron microscopy.**

We fixed the tissue with 2.5% (v/v) glutaraldehyde in a buffered solution of 0.1 M sodium cacodylate buffer, pH 7.3, for 2 h at room temperature. We washed this fixed tissue (three times; 10–15 min each) with fresh buffer and post-fixed with 1% osmium tetroxide buffered with 0.1 M sodium cacodylate, pH 7.3, for 1 h with gentle agitation every 10 min at 25 °C. After osmium tetroxide post-fixation, we washed the tissue again three times with fresh buffer as above. We then dehydrated specimens with a series of ethanol solutions of increasing concentration, beginning with 50% and progressing through 70%, 80%, 95% and 100% absolute ethanol. We transferred from 100% ethanol to the Tousimis 780A Critical-Point Dryer and dried with $CO_2$. We sputter-coated samples with 10 nm AuPd (60%/40% alloy) using a Denton DV-502A high-vacuum system (sputter module used was Denton DSM-5; Denton Vacuum). We then visualized samples with a Hitachi S-900 scanning electron microscope. For transmission electron microscopy (TEM), we fixed and then post-fixed the tissue samples as above. We immersed the tissue in ultraclean absolute acetone and carefully dissected it into pertinent regions of interest from the anterior apex, keeping one dimension of the tissue at ~3 mm. We performed one 15-min incubation in absolute acetone before infiltrating in mixtures of acetone and Poly Bed 812 resin (Polysciences) of increasing concentrations. We then oriented the specimens, positioned them in labeled molds and placed them in an oven for curing. We trimmed the hardened blocks and prepared semithin sections, 1.0–1.5 μm, with glass knives; we mounted sections on microscope slides and stained them with toluidine blue for 1 min at 80 °C. We examined the sections with light microscopy, and if an appropriate area for electron microscopy was found, we trimmed the block to the selected area. We mounted ultrathin sections of 55–65 nm on copper grids and stained with uranyl acetate and lead citrate. We used a Reichert Ultracut S Ultramicrotome (Leica-Microsystems) for both semithin and ultrathin sectioning. We performed ultrathin sectioning with a diamond knife. After making ultrathin sections, we cut a semithin section, mounted it on a glass slide and stained it with toluidine blue as before to correlate structures at the light and electron microscopic levels. We examined the stained ultrathin sections with a JEOL-1200 EXII transmission electron microscope. We recorded images with a SIS MegaView III high resolution CCD camera.

*Note:* ***Supplementary information*** *is available on the Nature Medicine website.*

**Author contributions**

H.C.O. and D.A.T. conceived, designed and oversaw all of the studies, collection of results, interpretation of data and writing of the manuscript. H.C.O. was responsible for the primary undertaking, completion and supervision of all studies during his tenure at the University of Minnesota. T.S.M. designed and implemented the bioreactor studies along with H.C.O., participated in the mechanical testing studies and was instrumental in data and figure preparation for the final manuscript. S.-K.G. performed most of the immunohistochemistry and staining, except for the re-endothelialized tissues. L.D.B. performed the mechanical testing. S.M.K. decellularized the hearts, performed all surgeries and re-endothelialization experiments, and participated in the bioreactor studies. T.I.N. performed the motion analysis of the movies.

## Acknowledgments

We thank S. Keirstead and D. Lowe for access to electromechanical stimulation equipment and guidance; J. Sedgewick and J. Oja of the Biomedical Image Processing Laboratory at the University of Minnesota, Minneapolis, for access to photographic equipment and technical support; and the staff of the University of Minnesota CharFac facility, especially A. Ressler, for TEM assistance. This study was supported by a Faculty Research Development Grant to H.C.O. and D.A.T. from the Academic Health Center, University of Minnesota, Minneapolis, and by funding from the Center for Cardiovascular Repair, University of Minnesota, and the Medtronic Foundation to D.A.T.

Received 29 May 2007; Accepted 18 October 2007; Published online 13 January 2008.

## References

1. Kobashigawa, J.A. & Patel, J.K. Immunosuppression for heart transplantation: where are we now? *Nat. Clin. Pract. Cardiovasc. Med.* **3**, 203–212 (2006). | **Article** | **PubMed** | **ChemPort** |
2. Eschenhagen, T. & Zimmermann, W.H. Engineering myocardial tissue. *Circ. Res.* **97**, 1220–1231 (2005). | **Article** | **PubMed** | **ISI** | **ChemPort** |
3. Zimmermann, W.H. *et al.* Engineered heart tissue grafts improve systolic and diastolic function in infarcted rat hearts. *Nat. Med.* **12**, 452–458 (2006). | **Article** | **PubMed** | **ChemPort** |
4. Sekine, H., Shimizu, T., Kosaka, S., Kobayashi, E. & Okano, T. Cardiomyocyte bridging between hearts and bioengineered myocardial tissues with mesenchymal transition of mesothelial cells. *J. Heart Lung Transplant.* **25**, 324–332 (2006). | **Article** | **PubMed** |
5. Robinson, K.A. *et al.* Extracellular matrix scaffold for cardiac repair. *Circulation* **112**, I135–I143 (2005). | **Article** | **PubMed** |
6. Radisic, M., Deen, W., Langer, R. & Vunjak-Novakovic, G. Mathematical model of oxygen distribution in engineered cardiac tissue with parallel channel array perfused with culture medium containing oxygen carriers. *Am. J. Physiol. Heart Circ. Physiol.* **288**, H1278–H1289 (2005). | **Article** | **PubMed** | **ChemPort** |
7. Furuta, A. *et al.* Pulsatile cardiac tissue grafts using a novel three-dimensional cell sheet manipulation technique functionally integrates with the host heart, *in vivo*. *Circ. Res.* **98**, 705–712 (2006). | **Article** | **PubMed** | **ChemPort** |
8. Miyagawa, S. *et al.* Tissue cardiomyoplasty using bioengineered contractile cardiomyocyte sheets to repair damaged myocardium: their integration with recipient myocardium. *Transplantation* **80**, 1586–1595 (2005). | **Article** | **PubMed** | **ChemPort** |
9. Park, H., Radisic, M., Lim, J.O., Chang, B.H. & Vunjak-Novakovic, G. A novel composite scaffold for cardiac tissue engineering. *In Vitro Cell. Dev. Biol. Anim.* **41**, 188–196 (2005). | **Article** | **PubMed** | **ChemPort** |
10. Dellgren, G., Eriksson, M.J., Brodin, L.A. & Radegran, K. Eleven years' experience with the Biocor stentless aortic bioprosthesis: clinical and hemodynamic follow-up with long-term relative survival rate. *Eur. J. Cardiothorac. Surg.* **22**, 912–921 (2002). | **Article** | **PubMed** |

11. Rieder, E. *et al.* Decellularization protocols of porcine heart valves differ importantly in efficiency of cell removal and susceptibility of the matrix to recellularization with human vascular cells. *J. Thorac. Cardiovasc. Surg.* **127**, 399–405 (2004). | **Article** | **PubMed** |

12. Ketchedjian, A. *et al.* Recellularization of decellularized allograft scaffolds in ovine great vessel reconstructions. *Ann. Thorac. Surg.* **79**, 888–896 (2005). | **Article** | **PubMed** |

13. Chen, R.N., Ho, H.O., Tsai, Y.T. & Sheu, M.T. Process development of an acellular dermal matrix (ADM) for biomedical applications. *Biomaterials* **25**, 2679–2686 (2004). | **Article** | **PubMed** | **ChemPort** |

14. Gilbert, T.W., Sellaro, T.L. & Badylak, S.F. Decellularization of tissues and organs. *Biomaterials* **27**, 3675–3683 (2006). | **PubMed** | **ChemPort** |

15. Gerecht-Nir, S. *et al.* Biophysical regulation during cardiac development and application to tissue engineering. *Int. J. Dev. Biol.* **50**, 233–243 (2006). | **Article** | **PubMed** |

16. Ossipow, V., Laemmli, U.K. & Schibler, U. A simple method to renature DNA-binding proteins separated by SDS-polyacrylamide gel electrophoresis. *Nucleic Acids Res.* **21**, 6040–6041 (1993). | **Article** | **PubMed** | **ChemPort** |

17. Paszek, M.J. *et al.* Tensional homeostasis and the malignant phenotype. *Cancer Cell* **8**, 241–254 (2005). | **Article** | **PubMed** | **ISI** | **ChemPort** |

18. Johnson, P., Maxwell, D.J., Tynan, M.J. & Allan, L.D. Intracardiac pressures in the human fetus. *Heart* **84**, 59–63 (2000). | **Article** | **PubMed** | **ChemPort** |

19. Roy, S., Silacci, P. & Stergiopulos, N. Biomechanical properties of decellularized porcine common carotid arteries. *Am. J. Physiol. Heart Circ. Physiol.* **289**, H1567–H1576 (2005). | **Article** | **PubMed** | **ChemPort** |

20. Courtman, D.W. *et al.* Development of a pericardial acellular matrix biomaterial: biochemical and mechanical effects of cell extraction. *J. Biomed. Mater. Res.* **28**, 655–666 (1994). | **Article** | **PubMed** | **ChemPort** |

21. Mirsadraee, S. *et al.* Development and characterization of an acellular human pericardial matrix for tissue engineering. *Tissue Eng.* **12**, 763–773 (2006). | **Article** | **PubMed** | **ChemPort** |

22. Bodnar, E., Olsen, E.G., Florio, R. & Dobrin, J. Damage of porcine aortic valve tissue caused by the surfactant sodiumdodecylsulphate. *Thorac. Cardiovasc. Surg.* **34**, 82–85 (1986). | **PubMed** | **ChemPort** |

23. Grabow, N. *et al.* Mechanical and structural properties of a novel hybrid heart valve scaffold for tissue engineering. *Artif. Organs* **28**, 971–979 (2004). | **Article** | **PubMed** | **ChemPort** |

24. Russ, J. *The Image Processing Handbook* Ch 4. (CRC Press, London, 2002).

25. Press, W.H., Teukolsky, S.A., Vetterling, W.T. & Flannery, B.P. in *Numerical Recipies in C: The Art of Scientific Computing* Ch. 12 (Cambridge University Press, Cambridge, UK, 1992).

26. Ono, K. & Lindsey, E.S. Improved technique of heart transplantation in rats. *J. Thorac. Cardiovasc. Surg.* **57**, 225–229 (1969). | **PubMed** | **ISI** | **ChemPort** |

1. Department of Surgery, Massachusetts General Hospital, Harvard Medical School, 55 Fruit Street, Boston,

Massachusetts 02114, USA.
2. Center for Cardiovascular Repair, University of Minnesota, 312 Church Street Southeast, 7-105A NHH, Minneapolis, Minnesota 55455, USA.
3. Department of Biomedical Engineering, University of Minnesota, 312 Church Street Southeast, 7 NHH, Minneapolis, Minnesota 55455, USA.
4. Department of Integrative Biology and Physiology, University of Minnesota, 6-125 Jackson Hall, 312 Church Street Southeast, Minneapolis, Minnesota 55455, USA.

Correspondence to: Doris A Taylor[2,4] e-mail: **dataylor@umn.edu**



***Nature Medicine*** ISSN 1078-8956 EISSN 1546-170X